The Effect of Doping on the Electrophysical Properties of Polycrystalline Diamond Films Deposited from an Abnormal Glow Discharge

A V Kabyshev, F V Konusov, S A Linnik and G E Remnev
National Research Tomsk Polytechnic University, 30, Lenin Avenue, 634050, Tomsk, Russia

E-mail: konusov@hvd.tpu.ru, kabyshev@tpu.ru

Abstract. The paper is focused on the study of the boron doping effect on the electrical characteristics, on the mechanism of charge carrier transfer, and on the energy spectrum of the localized defect states in the polycrystalline diamond films (PDF) deposited from an abnormal glow discharge. PDF doping enables to form the semiconductor layers of p-type conductivity, which have as good properties as those of PDF produced by the alternative methods. The doping reduces the degree of disorder in the film material brought by the growth defects, which determine the film electrical characteristics and electrotransfer mechanism. The PDF electrical characteristics and electrotransfer mechanism are determined by the defects of different nature, whose band gap energy levels have a continuous energy distribution. A p-type activation component is realized in the exchange of charge carriers between the valence band and shallow acceptor levels with the activation energy of 0.013–0.022 eV. Doping increases the effect of the hopping mechanism of the conductivity involving the localized states with a density of (1–6)$\cdot 10^{20}$ $eV^{-1}\cdot cm^{-3}$ distributed near the Fermi level, which is in the low half of the band gap.

Keywords: polycrystalline diamond films, electrical conduction, photoconductivity, localized states of defects

1. Introduction

The unique chemical, mechanical, electrical and thermophysical, optical and photoelectrical properties of a diamond contribute to its wide application in high-frequency and high-temperature electronics [1–5]. Due to the limited potentials for application of diamond single crystals and epitaxial diamond films caused by their high cost, the most appropriate instruments are the polycrystalline diamond films (PDF), which are obtained by well-studied methods of the gas-phase deposition [1–9]. Not only dielectric PDF are used for these purposes (electrical conduction $\sigma=10^{-15}$–10^{-11} $S\cdot cm^{-1}$), but also high-conductivity films of n– and p–type obtained by doping during deposition with dopant atoms of nitrogen [1, 7, 10–12] and boron [1, 2, 13–16]. Doping with B atoms with a concentration of 10^{17}–$3\cdot 10^{21}$ cm^{-3} causes the high-conductivity layers of p–type with $\sigma=10^{-10}$–$3\cdot 10^{2}$ $S\cdot cm^{-1}$ [1, 7, and 13–16] and with the altered optical properties [1, 2, 17]. The use of such doped layers makes it possible to significantly increase the photoelectrical characteristics of the devices [1, 17–20]. The features of the formed polycrystalline structure of the films and the content of the growth defects influence the electrical characteristics of the deposited semiconductor layers. It stimulates the study of the impact of the deposition conditions on the electrical and photoelectrical properties of PDF. The method of the film deposition from abnormal glow discharge (AGD) plasma stands out among various methods of PDF deposition – using microwave discharge plasma, hot filament, and plasma-arc CVD. The efficiency of the method of PDF deposition from AGD plasma compared to the alternative ones is in its simplicity and a high growth rate [3, 4].

The aim of the work is to study the effect of boron doping on the electrical characteristics, on the dominant transfer mechanism, and on the energy spectrum of the defect localized states in PDF deposited from AGD plasma.

2. Research methods

The methods of film deposition from AGD and the study of the film structural features are described in detail in [3 and 4]. The dark surface conductivity σ and photoconductivity $\Delta\sigma_{ph}=\sigma_{ph}-\sigma$ (σ_{ph} is conductivity under lighting), photosensitive $K(U, T, h\nu)=\Delta\sigma_{ph}/\sigma$ were measured at a constant voltage across the electrodes U=0.01–300 V, at temperature T=300–700 K, and photon energy $h\nu$=1.5–4.0 eV [18]. The electrodes were deposited on the surface by rubbing the soft graphite. The temperature dependences of σ, $\Delta\sigma_{ph}(T)$ were approximated by the equation for the activation mechanism

$$\sigma_a(T) = \sigma_0 \times e^{(-\varepsilon_\sigma / k \cdot T)}, \qquad (1)$$

where σ_0 is a pre–exponential factor, ε_σ is an activation energy, k is the Boltzmann constant and by the equation for the hopping mechanism of transfer between the localized states (LS) near the Fermi level E_F in the band gap (BG) in the Mott model

$$\sigma_p(T) = \sigma'_0 \times e^{(-(T_0/T)^{0.25})}, \qquad (2)$$

where σ'_0 is a pre–exponential factor, T_0 is an activation energy [10, 11, 18]. The LS density $N(E_F)$ near the Fermi level was calculated from T_0 according to [18]. The sign of the dominant charge carriers was determined by the photo- and thermostimulated current amplitude $I_{PhTSC}(T, h\nu, U=0)$ [18].

3. Results and discussion

Current voltage characteristic (CVC) I(U), field dependence of K(U) and carrier transfer energy characteristics ε_σ, σ_0, T_0, σ'_0, $N(E_F)$, and I_{PhTSC} in the undoped low-conductivity ($\sigma=10^{-14}$–10^{-4} S) films deposited on the silicon substrate or separated from it vary in thickness and PDF deposition plane, due to the inhomogeneity of the PDF properties (figure 1). The variation in the electrical parameters of the deposited films may be caused by the heterogeneity in the crystallite size distribution and by the growth defects in their volume and at the boundaries or by the influence of hydrogen impurity in the surface layers that is proved by the analysis of [2, 12, 14–18, 20]. The differences of I(U) and K(U) are recorded from the growth smooth and the opposite rough sides (figure 1) [18]. The conductivity in the PDF separated from substrate from the growth side is higher than from the side of the substrate and the ratio between K is opposite (figure 1) [18]. In the films with $\sigma \lesssim 10^{-4}$ S, the deviation from the linear law is fixed: CVC obeys the exponential equation $I \propto \exp(\beta U)$ (β=0.02–0.06) or the power law $I \propto U^\alpha$ (α=1.2–3.3) (figure 1, curves 5, 7–9). This indicates the current effect limited by the space charge as in [12, 17, and 18]. With σ decreasing from 10^{-7} to 10^{-14} S, the parameters of nonlinearity increase from α=1.2 to α=3.3 and from β=0.02 to β=0.06. This indicates the increase in the variation in LS population caused by the increase in the content of defects in PDF. The value of the photoconductivity (K=0.1–1.0) and the nature of its field dependence K(U) strengthen the ratios between CVC [18]. The CVC and K(U) characteristics are determined by the inhomogeneous spatial distribution of the energy barrier that exists on the border of PDF with the electrodes and on the intercrystallite boundaries [8, 9, 12, 17, and 18]. Both in the center of the deposition and from the growth side, the CVC of the films with a conductivity $\sigma \gtrsim 10^{-4}$ S are almost linear (α=1.05–1.15) (figure 1, curve 6), photosensitivity of these films is low (K=0.003–0.05), and the field dependence of K(U) is low as shown in [18].

Regarding the substrate, the undoped film on the Si substrate with $\sigma=(1–2)\cdot10^{-5}$ S and the

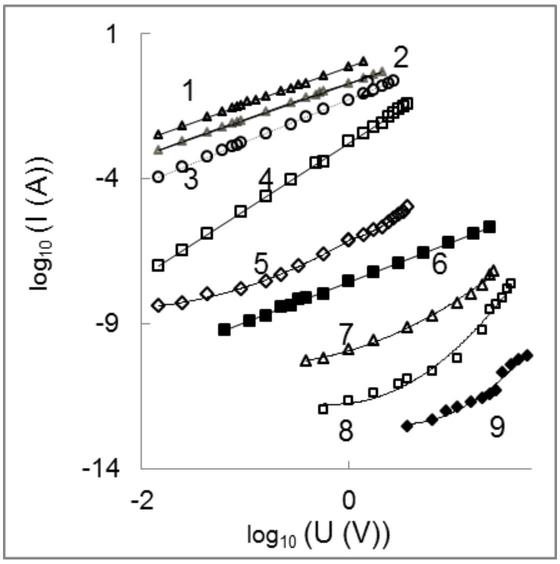

Figure 1. CVC of the films doped with boron and deposited on Si (1 and 2), Si substrate (3); CVC of the undoped PDF on Si (5) and Si substrates (4); CVC of the films separated from the substrate (6–9) for the surface (1, 3–9) and bulk conductivity (2) from the growth side (1, 5, 6, 8) and from the substrate side (7, 9) in the center (5–7) and on the edge of deposition (8, 9).

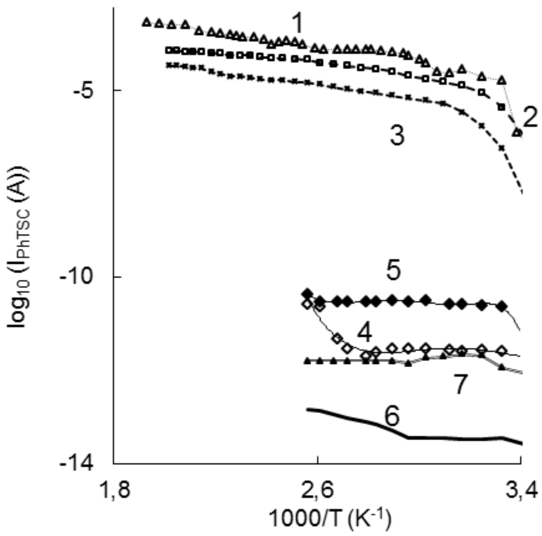

Figure 2. Temperature dependencies $I_{PhTSC}(T)$ in the dark (1–3, 4, 6) and under lighting (5, 7) in the doped PDF on Si in consecutive measurements (1, 2), in the substrate (3), in the undoped PDF on Si (4, 5) and in PDF separated from the substrate (6, 7).

coefficient α=1.85 of CVC possesses a lower conductivity $\sigma=2\cdot10^{-7}$ S and CVC higher nonlinearity (α=2–2.3, β=0.3–0.4) (figure 1, curves 4 and 5), as well as unstable photoconductivity [18]. The ratio between CVC and K(U) of the film and the substrate indicates the independence of the PDF and substrate properties that is determined by the decrease in σ by 2–4 orders from the layers from the growth side to the layers near the substrate, as for the most of the films separated from the substrates (figure 1, curves 6–9). In the film doped with boron on the ohmic Si substrate (α=1), CVC obeys almost linear law with α=1.05–1.1 for the bulk and surface conductivity, that reveals a weak influence of various heterogeneities, which are typical to the undoped films, on the conductivity (figure 1, curves 1–3). This conclusion is verified by a very low photosensitivity of the film $K \lesssim 10^{-4}$.

In the most low-conductivity undoped films with $\sigma \lesssim 10^{-7}$ S, n-type of σ and σ_{ph} dominates, as thermo and photostimulated currents $I_{PhTSC}(T)$ show [18]. Temperature dependences of σ, $\sigma_{ph}(T)$ within the interval T=300–720 K are determined by the thermostimulated electron exchange between shallow donor levels with the activation energy $\varepsilon_\sigma \lesssim 0.21$ eV and the conduction band (CB) (figure 2 and 3) [18]. Donor domination in the electrotransfer is most likely caused by the effect of the nitrogen-containing centers formed in PDF involving residual impurity of nitrogen in the reactor. The values of ε_σ in the deposited PDF indicate a weak population of electrically active LS, which is in 10^3–10^6 times lower compared to single crystals and epitaxial PDF. The ε_σ activation levels which are typical to diamond do not occur, as in [2, 7–11, 14, 16, 20]. We cannot exclude the effect of the holes exchange between LS of the defects and the valence band (VB) on the CVC, $\sigma(T)$ and K(U, hν) of the undoped films [18, 20]. It is verified by thermo- and photostimulated currents (figure 2, curves 4, 6 and 5, 7). The comparison of $I_{PhTSC}(T)$ for the films on the substrate and the films separated from it enables to eliminate the impact of the substrate on the thermoactivation of the holes (figure 2). In the doped film, $\sigma(T)$ is determined by the thermoactivated hole exchange between VB and shallow acceptor levels with an energy of $\varepsilon=\varepsilon_v$+(0.013–0.022) eV ($\varepsilon_v$ is a top of VB) (figures 2 and 3). It is

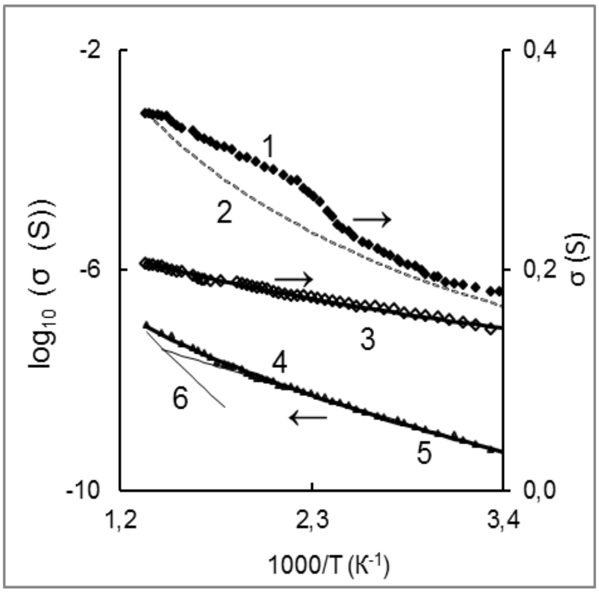

Figure 3. Temperature dependences of σ(T) of doped PDF on the Si substrate before (1), after annealing to 730 K (3) and undoped PDF on the Si substrate (4) and their approximation with the equations of hopping (2) (2, 3) and activation conductivity (1) (5, 6) at $T_0^{0.25}$=23.7 $K^{0.25}$, σ'_0=943 S (2); 16.01 $K^{0.25}$, 121 S (3); ε_σ=0.19 eV, σ_0=8.7·10^{-7} S (5), 0.6 eV, 9·10^{-4} S (6).

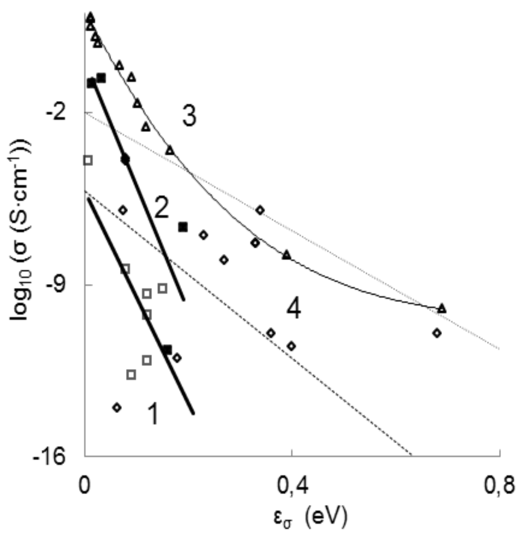

Figure 4. Interrelation between conductivity σ of the films and its activation energy ε_σ in the deposited films separated from the substrate (1) (□), in the films on the silicon substrate (2) (■) and in the other PDF reported by [16] (3) (Δ) and [2, 7, 10, 11, and 14] (band 4) (◊).

typical for PDF doping by boron impurity, as shown in [1, 13, 14, 16, 17]. The conclusion is verified by the near values of ε_σ for σ(T) and I_{PhTSC}(T) (figures 2 and 3).

The electrical parameters and the ratio between them indicate the effect on the hopping conductivity transfer that is verified by the approximation σ(T) by the Eq. (2) within the interval T=300–700 K (figure 3) is typical for PDF [7–11, 17, 18]. LS density calculated from the dependence σ(T) for the undoped PDF is $N(E_F)=10^{17}$–10^{21} $eV^{-1}\cdot cm^{-3}$ [18]. The typical LS density for the other PDF is $N(E_F)$=(4–8)·10^{19} [10, 11] and 10^{15}–10^{18} $eV^{-1}\cdot cm^{-3}$ [17]. The Fermi level is located in a lower part of BG close to the VB by analogy with the data in [1, 13, 17]. The value of the most probable jump distance calculated according to [10, 11, and 18] with the values $N(E_F)$ is R=1–10 nm. Boron doping enhances the approximation of σ(T) by Eq. (2), that indicates the increase in the effect of σ_p to the electrotransfer (figure 3). The density of LS distributed near E_F after doping is (1–6)·10^{20} $eV^{-1}\cdot cm^{-3}$, and a jump distance R=1.4–2.1 nm.

The dependences σ(T) and parameters K, ε_σ, σ_0, T_0, σ'_0, $N(E_F)$ indicate the presence of the activation and hopping mechanisms, whose effect on the electrotransfer varies during the variation of deposition conditions (figures 3–6). In the undoped PDF on the Si substrate, σ(T) is approximated separately by the Eq. (1) or (2), but more accurately by the sum of two activation components $\sigma(T)=\sigma_{a1}(T)+\sigma_{a2}(T)$ or by the sum of the activation and hopping components $\sigma(T)=\sigma_p(T)+\sigma_{a2}(T)$ (figure 3). The decomposition of curves σ(T) for the sum of components confirms the impact on the properties of the deep levels with $\varepsilon_\sigma \gtrsim$ 0.6 eV induced by the more stable defects. In the PDF doped with boron after heating up to 720 K, the nonequilibrium component of conductivity disappears due to the annihilation of unstable acceptor defects, LS density being increased from 1.2·10^{20} to 5.9·10^{20} $eV^{-1}\cdot cm^{-3}$, meanwhile a jump distance decreases from 2.1 to 1.4 nm (figure 3).

The correlation between the parameters of the activation and hopping components enable to additionally specify a predominant transfer mechanism. The interrelations between the photosensitivity K, conductivity σ, multiplier factor σ_0, and activation energy ε_σ indicate a significant

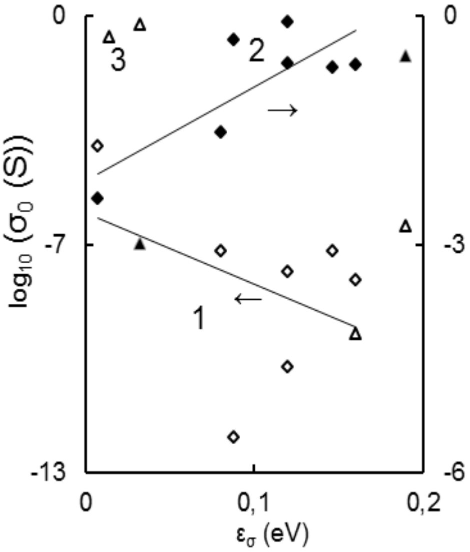

Figure 5. σ_0 vs. ε_σ (◇, Δ) (1, 3) and K vs. ε_σ (♦, ▲) (2) in the films separated from the substrate (◇,♦) and on the silicon substrate (Δ ▲).

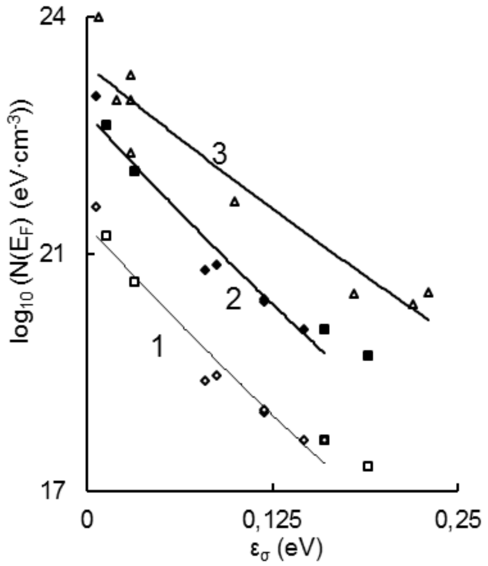

Figure 6. $N(E_F)$ vs. ε_σ in PDF separated from the substrate (◇, ♦) and on the Si substrate (□, ■) (1, 2). The data are given for UNCD (Δ) (3) [10]. Attenuation constant α=5.7·10^6 (1) and 2·10^7 cm^{-1} (2).

role of activation transport in PDF (figures 4 and 5). The role of the hoping component of the electrotransfer in PDF deposited from AGD is higher than in the other CVD films, as the dependencies $\sigma(\varepsilon_\sigma)$ show (figure 4). The correlation between σ and ε_σ for the AGD films on the Si substrate and the films separated from it is slightly different. The values σ and ε_σ boron-doped films are separated from those in the undoped and nitrogen-doped PDF (figure 4). In the boron-doped PDF deposited from AGD on the Si substrate, the values σ and ε_σ are located near these values (curve 2) that corresponds to the concentration of boron atoms in the films (0.3–3)·10^{20} cm^{-3} according to [16]. The multiplier factor σ_0 significantly exceeds its values for the undoped films due to the increase of the σ_p effect (figure 5, curve 1 and points 3). The correlation $K(\varepsilon_\sigma)$ (figure 5, curve 2) indicates the predominance of the activation mechanism of photoconductivity [18]. Besides, this correlation shows that the content of photosensitive defects in the undoped PDF on the substrate is lower than in the films separated from it. In the doped films this transfer mechanism of the light-activated holes is lacking, as shown by the low photosensitivity $K \leq 10^{-4}$ and curves $I_{PhTSC}(T)$ (figure 2).

The correlation $N(E_F)(\varepsilon_\sigma)$ in PDF deposited by AGD and by the other methods is typical for noncrystalline semiconductors possessing a high concentration of defects (figure 6) [10, 11, 17, 18]. The effect of the substrate is insignificant. The data for the doped PDF form a total array with the undoped films. By analogy with the approach developed in [1, 8–11, and 13–17], we concluded in [18], that in the undoped PDF hopping transfer σ_p on the LS near E_F dominates over the activated σ_a within the interval T=300–500 K. The invert correlation in favour of the activation component involving LS defects in the region of the “tails” of the allowed bands occurs when T=500–700 K. During the film doping, the range of the σ_p component dominance is expended to T=300–700 K, as shown by the approximation $\sigma(T)$ (figure 3) and the correlation $\sigma(\varepsilon_\sigma)$ (figure 4). When T>600 K, the effect of the potential barrier between crystallites is increased [18]. The correlation between the values

σ, ε_σ, and BG width, calculated form the absorption spectra agree with developed transfer models, the transfer being realized through the charge carrier exchange between BG and LS through the mobility gap [1 and 18].

4. Conclusion

The doping of the polycrystal diamond films with the impurity atoms of boron during the deposition from abnormal glow discharge enables to form the semiconductor layers with p-type of conduction on the silicon substrate that have as good properties as PDF obtained by the alternative methods. The bottom low-conducting PDF layers isolate the upper conducting layers from the influence of the substrate. The vacuum annealing of the films up to 720 K stabilize the electrical characteristics. The doping diminishes the degree of film material disordering by the growth defects compared to the undoped films that affects the electrical and photoelectrical characteristics and the conductivity mechanism. The activation component of the p–type conductivity is realized in the exchange of charge carriers between the VB and shallow acceptor levels with the activation energy of 0.013–0.022 eV. Doping increases the effect of the hopping mechanism of the conductivity involving the LS defects with a density of up to $(1–6)\cdot 10^{20}$ $eV^{-1}\cdot cm^{-3}$ near the Fermi level located in the low half of the BG.

Acknowledgments

The work is performed within the megaproject of Tomsk Polytechnic University (VIU_IFVT_85_2014) "Materials for Extreme Conditions"

References

[1] Williams O A 2011 *Diamond and Relat. Mater.* **20** 621
[2] Polyakov V I, Rukovishnikov A I, Avdeeva L A, Kun'kova Z E, Varnin V P, Teremetskaya I G and Ralchenko V G 2006 *Diamond and Relat. Mater.* **15** 1972
[3] Linnik S A and Gaydaychuk A V 2013 *Diamond and Relat. Mater.* **32** 43
[4] Linnik S A and Gaydaychuk A V 2012 *Tech. Phys. Lett.* **38** 258
[5] Bevilacqua M and Jackman R B 2009 *Appl. Phys. Lett.* **95** 243501
[6] Ueda K, Kawamoto K, Soumiya T and Asano H 2013 *Diamond and Relat. Mater.* **38** 41
[7] Chiquito A J, Berengue O M, Diagonel E and Galzerani J C 2007 *J. Appl. Phys.* **101** 033714
[8] Kopylov P G, Lotonov A M, Apolonsky I A and Obraztzov A N 2009 *Vestn. of MSU.Ser.3(in russian)* 2 54
[9] Trucchi D M, Cappelli E, Conte G, Mattei G, Gramaccioni C and Ascarelli P 2005 *Diamond and Relat. Mater.* **14** 575
[10] Achatz P, Williams O A, Bruno P, Gruen D M, Garrido A and Stutzmann M 2006 *Phys. Rev.* **B 74** 155429
[11] Gan L, Bolker A, Saguy C, Kalish R, Tan D L, Tay B K, Gruen D and Bruno P 2009 *Diamond and Relat. Mater.* **18** 1118
[12] Conte G, Rossi MC, Spaziani F and Arcangeli R 2005 *Diamond and Relat. Mater.* **14** 570
[13] Hikavyy A, Clauws P, Maes J, Moshchalkov V V, Butler J E, Feygelson T, Williams O A, Daenen M and Haenen K 2006 *Phys. status solidi* **A 203** 3021
[14] Muret P and Saby Ch 2004 *Semicond. Sci. and Technol.* **19**1
[15] Hubik P, Mares J J, Kozak H and Kromka A 2012 *Diamond and Relat. Mater.* **34** 63
[16] Gajewski W, Achatz P, Williams O A, Haenen K, Bustarret E, Stutzmann M, and Garrido J A 2009 *Phys. Rev.* **B 79** 045206
[17] Nath S and Wilson J I B 1996 *Diamond and Relat. Mater.* **5** 65
[18] Konusov F V, Kabyshev A V, Linnik S A, Gaydaychuk A V and Remnev G E 2014 *J. of Phys.: Conf. ser.* **552** 012046
[19] Chaudhary A, Welch J O and Jackman R B 2010 *Appl. Phys. Lett.* **96** 242903
[20] Ri Sung-Gi, Takeuchi Daisuke, Kato Hiromitsu, Ogura Masahiko, Makino Toshiharu, Yamasaki Satoshi, Okushi H, Rezek B and Nebel Ch E 2005 *Appl. Phys. Lett.* **87** 262107